



Contents lists available at ScienceDirect

Biochimica et Biophysica Acta

journal homepage: www.elsevier.com/locate/bbamcr

The ratio of SRPK1/SRPK1a regulates erythroid differentiation in K562 leukaemic cells

Ioannis Sanidas^a, Vassiliki Kotoula^b, Eleni Ritou^c, Jasmijn Daans^d, Christof Lenz^e, Mario Mairhofer^f, Makrina Daniilidou^a, Andrea Kolbus^f, Volker Krufft^e, Peter Ponsaerts^d, Eleni Nikolakaki^{a,*}

^a Laboratory of Biochemistry, Department of Chemistry, The Aristotle University, 54124, Thessaloniki, Greece

^b Department of Pathology, School of Medicine, The Aristotle University, 54124, Thessaloniki, Greece

^c Laboratory of Biological Chemistry, Medical School, The University of Ioannina, 45110, Ioannina, Greece

^d Laboratory of Experimental Hematology, Faculty of Medicine, University of Antwerp, B-2610 Antwerp, Belgium

^e Applied Biosystems, Frankfurter Str. 129B, 64293 Darmstadt, Germany

^f Department of Obstetrics and Gynecology, Medical University of Vienna, Vienna, A-1090, Austria

ARTICLE INFO

Article history:

Received 21 December 2009

Received in revised form 19 July 2010

Accepted 26 July 2010

Available online 12 August 2010

Keywords:

SRPK1a

SRPK1

K562 cell

Differentiation

Erythroid progenitor cell

ABSTRACT

SRPK1, the prototype of the serine/arginine family of kinases, has been implicated in the regulation of multiple cellular processes such as pre-mRNA splicing, chromatin structure, nuclear import and germ cell development. SRPK1a is a much less studied isoform of SRPK1 that contains an extended N-terminal domain and so far has only been detected in human testis. In the present study we show that SRPK1 is the predominant isoform in K562 cells, with the ratio of the two isoforms being critical in determining cell fate. Stable overexpression of SRPK1a induces erythroid differentiation of K562 cells. The induction of globin synthesis was accompanied by a marked decrease in proliferation and a significantly reduced clonogenic potential. Small interfering RNA-mediated down-regulation of SRPK1 in K562 cells results similarly in a decrease in proliferative capacity and induction of globin synthesis. A decreased SRPK1/SRPK1a ratio is also observed upon hemin/DMSO-induced differentiation of K562 cells as well as in normal human erythroid progenitor cells. Mass spectrometric analysis of SRPK1a-associated proteins identified multiple classes of RNA-binding proteins including RNA helicases, heterogeneous nuclear ribonucleoproteins, ribosomal proteins, and mRNA-associated proteins. Several of the SRPK1a-copurifying proteins have been previously identified in ribosomal and pre-ribosomal complexes, thereby suggesting that SRPK1a may play an important role in linking ribosomal assembly and/or function to erythroid differentiation in human leukaemic cells.

© 2010 Elsevier B.V. All rights reserved.

1. Introduction

Serine/Arginine protein kinases (SRPKs) that phosphorylate SR/RS dipeptide-containing proteins have been conserved throughout evolution and so far approximately 15 distinct genes encoding members of this family have been identified in the genomes of mammals, yeast, fruit fly, nematode, and plants [1,2].

Abbreviations: SR, serine/arginine; RS, arginine/serine; SRPK, serine/arginine protein kinase; LBR, lamin b receptor; SAFB1, scaffold attachment factor B1; Hsp, Heat shock protein; EGFP, enhanced green fluorescent protein; EPO, erythropoietin; LC, liquid chromatography; DHX9, DEAH (Asp-Glu-Ala-His) box polypeptide; DDX21, DEAD (Asp-Glu-Ala-Asp) box polypeptide; HNRNP, heterogeneous nuclear ribonucleoprotein; MOV, Moloney leukaemia virus; MATR3, matrin 3; PABP, poly(A) binding protein; IGF2BP, insulin-like growth factor 2 mRNA binding protein; SYNCRIP, synaptotagmin binding, cytoplasmic RNA interacting protein; RP, ribosomal protein; NPM, nucleophosmin; CREB, cAMP response element binding protein

* Corresponding author. Laboratory of Biochemistry, Department of Chemistry, Aristotle University of Thessaloniki, 541 24 Thessaloniki, Greece. Tel.: +30 2310 997726; fax: +30 2310 997689.

E-mail address: nikol@chem.auth.gr (E. Nikolakaki).

The SRPK family is represented by four members in humans: SRPK1 (named also SRPK1 isoform 2 according to UniProtKB/Swiss-Prot Q96SB4), SRPK1a (named also SRPK1 isoform 1 according to UniProtKB/Swiss-Prot Q96SB4), SRPK2 and SRPK3. SRPK1 was mapped to chromosome 6p21.2–p21.3 [3]. Splicing out of a 513-bp segment, which is located between the first two exons of the SRPK1 locus, results in the production of SRPK1, whereas splicing in of the 513-bp segment yields its isoform SRPK1a [2]. SRPK1 is predominantly expressed in testis, but is also present in detectable levels in most tissues [4,5] (see also Gene Expression Atlas databank, <http://expression.gnf.org/cgi-bin/index.cgi>), while so far SRPK1a was only seen in testis [2]. SRPK2 was mapped to chromosome 7q22–q31.1 [3] and its levels are high in testis and brain [5] (see also Gene Expression Atlas). SRPK3 (also known as STK23) is specifically expressed in the heart and skeletal muscle [1]. SRPK3-null mice display type 2 fiber-specific myopathy with a marked increase in centrally placed nuclei, while transgenic mice overexpressing SRPK3 showed severe myofiber degeneration and early lethality [1].

The vast majority of the functional studies concerning mammalian SRPKs was based on SRPK1. SR proteins that mediate both constitutive and alternative splicing of pre-mRNAs, lamin B receptor (LBR), an integral protein of the inner nuclear membrane and protamine 1, a small basic arginine-rich protein that replaces histones during the development of mature spermatozoa, have been the most extensively studied cellular substrates of SRPK1 [4–8]. Phosphorylation of SR proteins is required for their recruitment to sites of transcription [9,10], promotes spliceosome assembly [11], and mediates the interaction of SR proteins with the C-terminal domain of polymerase II to coordinate transcription with splicing [10]. It has also been proposed that phosphorylation of SR proteins in the cytoplasm may act as a switch between mRNA unloading and SR protein reimport to the nucleus [12,13]. LBR is one of the key factors that have been implicated in chromatin anchorage to the nuclear envelope [14,15]. Takano et al. [16,17] have shown that SRPK1-mediated phosphorylation affects LBR association with chromatin. Phosphorylation of protamine 1 is required for its transient docking to the nuclear envelope, which is an important intermediate step that directs the proper deposition of protamine molecules into sperm chromatin [4,18,19].

Previous studies have shown that SRPK1, SRPK1a and SRPK2 are mainly localized in the cytoplasm and to a lesser extent in the nucleus, despite having putative nuclear localization signals [2,4,5,20,21]. A unique spacer sequence in each kinase, dividing conserved catalytic kinase domains into two halves, seems to be responsible for their cytoplasmic distribution [20]. It was recently shown that this spacer domain, together with yet uncharacterized SRPK1 sequences, mediate the attachment of the kinase to the Hsp70/Hsp90 machinery, thereby functioning as a docking motif to restrict SRPK1 in the cytoplasm [22]. Cytoplasmic SRPKs may be responsible for initial SR protein phosphorylation that is critical for their interaction with transportin and their subsequent import into the nucleus [13]. However, the presence of SRPKs in the cytoplasm may also reflect a variety of yet unidentified roles of these kinases, in addition to their nuclear functions. Interestingly, a cell cycle signal induces nuclear translocation of SRPK1 and its fission yeast homologue *dsk1* at the G_2/M boundary [20,23].

In the present study we noticed that SRPKs are highly expressed in different erythroid and lymphoid cell lines, with SRPK1 mRNA being far more abundant than SRPK1a. Using K562 human leukaemic cells as a model system, we demonstrated that the ratio of SRPK1/SRPK1a plays a decisive role in determining cell fate. Stable overexpression of SRPK1a or siRNA-mediated down-regulation of SRPK1 in K562 cells results in a substantial induction of globin synthesis. The observed erythroid differentiation is accompanied by growth inhibition and a significantly reduced clonogenic potential, as compared to the parental cells. A similar decreased SRPK1/SRPK1a ratio is also observed following hemin/DMSO-induced differentiation of K562 cells as well as in normal human erythroid progenitor cells. Over-expressed SRPK1a was found to localize in the P100 fraction, cytoplasm and nuclear matrix and associate with a variety of RNA binding proteins, many of which have been previously identified in pre-ribosomal and ribosomal complexes. In view of the fact that none of the proteins co-purifying with SRPK1a is directly phosphorylated by the kinase due to the lack of RS domain(s), we discuss the potential association of SRPK1a-containing complexes with erythroid differentiation.

2. Materials and methods

2.1. K562 and primary erythroid cells culture, induction of differentiation

K562 cells were maintained in RPMI medium supplemented with 10% (v/v) fetal calf serum with antibiotics. Cell growth was monitored by determining the cell number/ml with the use of a Coulter counter model ZBI. For induction of differentiation, exponentially growing

K562 cells were seeded at 1×10^5 cells/ml in the presence of 60 μ M hemin and 1.5% DMSO. The induction period was 4 days without changing the medium. Hemoglobin-containing cells were detected by staining the cells with a benzidine-peroxide solution [24].

Primary erythroid cells were isolated from cord blood as previously described [25]. Cells were maintained in StemSpan Serum-Free Expansion Medium (SFEM) (StemCell Technologies) supplemented with 2 U/ml erythropoietin (Janssen-Cilag, 10,000 U/ml), 100 ng/ml Stem Cell Factor, 10^{-6} M dexamethasone, 40 ng/ml Insulin-like Growth Factor-1 and 20 μ g/ml of a cholesterol-rich lipid mix (all from Sigma) at a concentration of approximately 2 million cells per ml. At day 14, more than 95% of the cells showed the characteristics of erythroid progenitors in haematological staining, cell diameter and flow cytometry (>95% of the cells were positive for CD71 and CD36). Terminal erythroid differentiation was induced on day 14 by seeding the cells in StemSpan SFEM supplemented with 10 U/ml erythropoietin, insulin 4×10^{-4} IE/ml (Actrapid, NovoNordisk 100 IE/ml), 10^{-6} M T3 thyroid hormone, 3×10^{-6} M mifepristone (RU486), 3% human serum (type AB, male) and 1 mg/ml transferrin (all from Sigma). Erythroid differentiation of the progenitors was monitored by accumulation of haemoglobin and size decrease (not shown).

2.2. Real Time PCR analysis

RNA was extracted from testis, various cancer cell lines and erythroid progenitor cells with TRIZOL according to standard procedures, subjected to DNase I treatment and purification with the RNeasy MinElute Cleanup Kit (Qiagen) and reverse transcribed with random hexamers and Superscript III (Invitrogen). All cDNA samples were normalized at 10 ng/ μ l (40 ng/20 μ l reaction). To assess the expression of SRPK1 and SRPK1a the following assays were designed with the Primer Express 3.0 software (Applied Biosystems): for SRPK1a (120 bp amplicon), sense primer: 5'-CTCCACATTCGCCCTT-CATC-3', antisense: 5'-CCTCGGTGCTGAGTTTCAGAT-3', probe: FAM-ATCCCTCTCTCTGAGTG-MGB; for SRPK1 (100 bp amplicon), sense primer: 5'-CACCATGGAGCGGAAAGTG-3', antisense: 5'-GCCTCGGTGCTGAGTT TCAG-3', probe: FAM-CCCGAAAGAAAAG-GACCA-MGB. Reactions were run in an ABI7500 real time PCR system equipped with the SDS software v1.4 (Biosolutions, Athens, GR). For normalization, we used *GUSB* in assays with testis and various cancer cell lines and *CSNK1D* in assays with primary erythroid cells. Based on the equal efficiency of the PCR assays (Supplementary Fig. 1), relative quantitation of SRPK1/SRPK1a mRNA was assessed with the $2^{-\Delta\Delta C_t}$ method, while relative changes of the two isoforms in K562-SRPK1a cells as compared to parental K562 cells were calculated automatically using the $2^{-\Delta\Delta C_t}$ method. In addition, the $2^{-\Delta\Delta C_t}$ method was used to evaluate the relative changes of SRPK1/SRPK1a mRNA during differentiation as compared to day 0 (start of differentiation), and also in K562 cells electroporated with a plasmid that expresses a short hairpin RNA targeting SRPK1 as compared to cells electroporated with a control construct. Samples were run in triplicate.

2.3. Construction of K562-SRPK1a stable cell line

For stable overexpression of SRPK1a in K562 cells, the pCMV2-FLAG-SRPK1a-IRES-EGFP plasmid was constructed. For this, the pIRES2-EGFP vector was digested with *Sall* and *XbaI*. A 1300-bp fragment was purified and cloned into the *Sall/XbaI* site of pCMV2-FLAG-SRPK1a plasmid [2]. K562 cells were co-electroporated with the pCMV2-FLAG-SRPK1a-IRES-EGFP plasmid and an empty pcDNA3-Neo^r plasmid (Invitrogen). To this end, 5×10^6 cells were resuspended in 500 μ l OptiMem medium (Invitrogen) supplemented with 10% FCS and transferred to a 4-mm electroporation cuvette. After addition of plasmid DNA (10 μ g of pCMV-FLAG-SRPK1a-IRES-EGFP plasmid and 1 μ g of pcDNA3-Neo^r plasmid), cells were electroporated at 260 V and

1050 μF using an EquiBio electroporation device. Next, cells were allowed to recover for 48 h before addition of 500 $\mu\text{g}/\text{ml}$ of the neomycin analogue G418 (Sigma). After 10 days of selection under G418, EGFP positive cells were sorted using a FACS-Vantage flow cytometer cell sorter (Becton Dickinson). After two additional weekly cell sorts for highly EGFP positive cells, the obtained cell line was named K562-SRPK1a. Cells were routinely analysed for EGFP expression and remained stable for more than 4 months.

2.4. Flow cytometric analysis of SRPK1a expression

K562 and K562-SRPK1a cells were processed for intracellular staining of over-expressed SRPK1a using an M5 anti-FLAG monoclonal antibody (Sigma) directed against the FLAG peptide sequence on the N-terminus of introduced SRPK1a. Briefly, cells (2×10^6 per staining) were fixed in 2% paraformaldehyde for 15 min at 4 °C, followed by permeabilization in 70% ethanol for 30 min at -20 °C. Next, both parental K562 and K562-SRPK1a cells were stained using an unconjugated M5 anti-FLAG antibody (1 $\mu\text{g}/100 \mu\text{l}$ cells in PBS) for 15 min at 4 °C. Following this, cells were washed twice and stained using a goat-anti-mouse (GAM) phycoerythrin (PE)-labelled secondary antibody (1 $\mu\text{g}/100 \mu\text{l}$ cells in PBS) for 15 min at 4 °C. Finally, cells were washed, resuspended in PBS and analyzed on a FACScan flow cytometer (Becton Dickinson) for EGFP expression (FL1-fluorescence) and SRPK1a over-expression (FL2-fluorescence). Data were analysed using WinMDI software.

2.5. Clonogenicity assay

K562 and K562-SRPK1a cells were harvested, washed three times in RPMI medium supplemented with 10% FCS, and plated (1000 cells) in 3 ml serum-free or serum-containing (10% FCS) 0.9% methylcellulose medium in 6-well plates with or without addition of 2 U/ml erythropoietin (EPO), following a previously optimized protocol [26]. The cultures were microscopically scored for colony formation after 14 days at 37 °C in 5% CO_2 in a fully humidified incubator. All experiments were performed in triplicate.

2.6. Creation of siRNA-encoding constructs

Plasmids encoding siRNAs targeting SRPK1 were generated using the siSTRIKE U6 Hairpin Cloning System (Promega) as described previously [27]. Briefly, sh4-SRPK1 encodes a siRNA targeting nucleotides 648 to 665 (5'-GATCATCAAATCCAATTA-3') of the human SRPK1 mRNA (NM_003137.3), while scr-SRPK1 encodes a scrambled version of this sequence (5'-ATCTACATGCATCATAA-3') and was used as control. Both the SRPK1 targeted and the control nucleotide, even though used before, were aligned against the Genebank database sequences to ensure specificity. Plasmids were purified using the Qiagen MaxiPrep protocol (Qiagen).

2.7. Immunofluorescence microscopy

Cells were collected by centrifugation, washed 3 times with phosphate-buffered saline (PBS) and allowed to adhere to Alcian blue-treated coverslips for 1 h. The samples were then fixed with 1% formaldehyde in PBS, permeabilized with 0.2% Triton X-100 and blocked with 0.5% fish skin gelatin. DNA staining (propidium iodide) and probing with the relevant primary (anti-SRPK1, anti-FLAG, both diluted 1:150) and secondary (FITC-conjugated goat anti-mouse, diluted 1:400; TRITC-conjugated goat anti-mouse, diluted 1:350) antibodies, was performed according to Maison et al. [28]. All secondary antibodies were purchased from Molecular Probes. Samples were visualized in a Leica SP confocal microscope.

2.8. Cell fractionation, western blotting and immunoprecipitation assays

Approximately 5×10^6 cells were harvested by centrifugation at 150g for 15 min, washed in phosphate-buffered saline (PBS), resuspended in 500 μl of ice-cold buffer A (10 mM Hepes-KOH pH 7.5, 10 mM KCl, 1.5 mM MgCl_2 , 0.5 mM DTT) and allowed to stand for 10 min at 4 °C. The cells were then collected by centrifugation as before, suspended in 200 μl of buffer A and lysed by 15 strokes of a glass Dounce homogenizer. The homogenate was centrifuged for 10 min at 4300g to yield a supernatant (S1) and a crude nuclear fraction. S1 was carefully decanted, mixed with 22 μl (0.1 volume) of buffer B (300 mM Hepes-KOH pH 7.5, 1.4 M KCl, 30 mM MgCl_2) and centrifuged at 10,000g for 10 min to yield a pellet (that practically did not contain any SRPKs) and a supernatant that was further fractionated into cytoplasmic (S100) and microsomal (P100) fractions by centrifuging at 100,000g for 60 min at 4 °C. The P100 pellets were resuspended in buffer A. The crude nuclear fraction was resuspended in 100 μl buffer A and laid onto a 1.2 ml cushion of 0.8 M sucrose in buffer A. After centrifugation at 4300g for 10 min, the pellet (purified nuclei) was collected, washed twice with PBS and further fractionated according to the protocol described by Jiang et al. [29] to yield a soluble nucleoplasmic, a DNase extracted and a remaining insoluble nuclear matrix fraction. Gel loading was adjusted to give equivalent cell numbers in each lane. Endogenous SRPK1/SRPK1a were detected by Western blotting, using an anti-SRPK1 monoclonal antibody recognizing both isoforms (BD Biosciences), while the M5 anti-FLAG monoclonal antibody was used for the detection of overexpressed FLAG-SRPK1a. To test the purity of the individual compartments a mouse monoclonal α -CREB (Cell Signaling) a polyclonal anti-lamin (α -L1) (kindly provided by Spyros Georgatos, Medical School, University of Ioannina) and a polyclonal antibody to ribosomal protein S6 (Acris Antibodies GmbH) were used.

Immunoprecipitations were performed with polyclonal antibodies against SRPK1 (recognizing both isoforms) and specifically against the N-terminal extended domain of SRPK1a [2]. *In vitro* phosphorylation assays were performed on beads as described previously using as substrate the N-terminal domain of LBR fused to GST (GST-LBRnt) [8]. Incorporation of radioactivity was measured by excising the respective radioactive bands from an SDS-PAGE gel and scintillation counting. RS kinase activity was expressed as total units (%).

For detecting hemoglobin or phosphorylated SR proteins, cells were lysed with 200 μl of 1% Triton buffer (1% Triton X-100, 50 mM Tris-HCl, pH 7.5, 150 mM NaCl, 10 $\mu\text{g}/\text{ml}$ aprotinin, and 1 mM PMSF) for 30 min on ice and passed 10 times through a 27-gauge needle. Cell extracts were clarified by centrifugation at 13,000g for 15 min in a microcentrifuge. Hemoglobin was detected by Coomassie blue staining, while the identity of phosphorylated SR proteins was confirmed by western blotting using the mAb104 monoclonal antibody (culture supernatant, kindly provided by Jamal Tazi, Institut de Génétique Moléculaire, C.N.R.S., Montpellier, France).

2.9. Immunoprecipitation of SRPK1a-associated proteins, mass spectrometry and data analysis

Approximately 10^8 K562-SRPK1a cells were lysed with 1.2 ml of 1% Triton buffer. The lysate was clarified by centrifugation, precleared by incubating with protein A-Sepharose for 3 h at 4 °C and immunoprecipitated with the anti-FLAG monoclonal antibody. Immunoprecipitates were analyzed by one-dimensional SDS-PAGE and stained with Coomassie blue. Specific bands were excised from the gel, cut into three pieces of equal size, washed, reduced, alkylated, and subjected to in-gel digestion with porcine trypsin as previously described [30]. Prior to analysis by nanoLC-MS/MS, the generated peptides were purified and concentrated using ZipTips (Millipore, Bedford, MA) according to the manufacturer's instructions.

Tryptic peptides were separated by nanoflow reversed phase-C18 chromatography on a Tempo 1D nanoLC system (Applied Biosystems) using a 90 min linear organic gradient on a 75 $\mu\text{m} \times 15 \text{ cm}$ RP-C18 column. The eluent was analyzed on a hybrid triple quadrupole/linear ion trap mass spectrometer (4000 Q TRAP™ LC/MS/MS System, Applied Biosystems) equipped with a nanoESI source and operated in information-dependent acquisition mode. An electrospray voltage of 2800 V, an interface heater temperature of 150 °C and a cone voltage of 60 V were used. The collision energy was dynamically adjusted according to the charge state and M_r of the precursors. Up to six MS/MS spectra per experimental cycle were acquired, resulting in an average duration of 3.6 s per cycle. Proteins were identified using the ProteinPilot 2.0.1 software with the PSPEP 0.99 Tool for false discovery calculation against a human International Protein Index protein sequence database (IPI, version 3.54, European Bioinformatics Institute, www.ebi.ac.uk/IPI/).

3. Results

3.1. Relative expression of SRPK1 and SRPK1a in various cancer cell lines

SRPK1 was originally purified and cloned from HeLa cells on the basis of its ability to phosphorylate members of the SR family of splicing factors [6,7], while SRPK1a was cloned from a human testis cDNA library and its extended N-terminal domain of 171 aminoacids was found to bind to the nuclear scaffold-associated protein SAFB1 [2]. To further probe into the biological function(s) of SRPKs, and if possible to discern the cellular activities displayed by the two isoforms, we first decided to assess the relative expression ratio of SRPK1/SRPK1a in various cancer cell lines, as well as in human testis that express high levels of SRPK1 [4]. To this end we performed relative quantitation analysis for the presence of SRPK1/SRPK1a transcripts in testis, HeLa, K562, Molt-4 and HL-60 cells. We chose

three leukaemia cell lines (K562, Molt-4 and HL-60 cells), since data from the Gene Expression Atlas databank (<http://expression.gnf.org/cgi-bin/index.cgi>), as well as from Northern blotting analysis, substantiate the high levels of expression of SRPK1 in different hematopoietic cell lines (Supplementary Fig. 2). In all cases, SRPK1 was by far the predominant isoform, with the relative ratio of SRPK1/SRPK1a mRNA ranging from 250 to 480 (Fig. 1). K562 cells express relatively high levels of SRPKs and therefore, we decided to use them in our subsequent studies. Our decision was also prompted by the fact that K562 cells have been largely employed in the past as a model system to study differentiation as well as to determine the therapeutic potential of new differentiating compounds.

3.2. Stable overexpression of SRPK1a promotes erythroid differentiation of K562 cells

In an attempt to bring to light the role of SRPK1a we decided to stably overexpress it in K562 cells. To this end we constructed the pCMV2-FLAG-SRPK1a-IRES-EGFP plasmid (see Materials and methods). The Internal Ribosome Entry Site (IRES) of the encephalomyocarditis virus (ECMV) permits the translation of both FLAG-SRPK1a and EGFP from a single bicistronic mRNA. K562 cells stably overexpressing SRPK1a and EGFP were selected by combined antibiotic selection and cell sorting as described in Materials and methods. Using flow cytometric analysis, it was shown that the majority (at least 70%) of the cultured K562-SRPK1a cell population expressed EGFP and could be co-stained with an anti-FLAG monoclonal antibody (Fig. 2A), while a FLAG-immunoreactive band was clearly visible in cell extracts of K562-SRPK1a cells (Fig. 2C, left panel). Immunoprecipitations using the specific anti-SRPK1a polyclonal antibody, followed by immunoblotting analysis of the immunoprecipitates with the anti-FLAG antibody, further confirmed the overexpression of SRPK1a (Fig. 2C, right panel). In addition, Real Time PCR

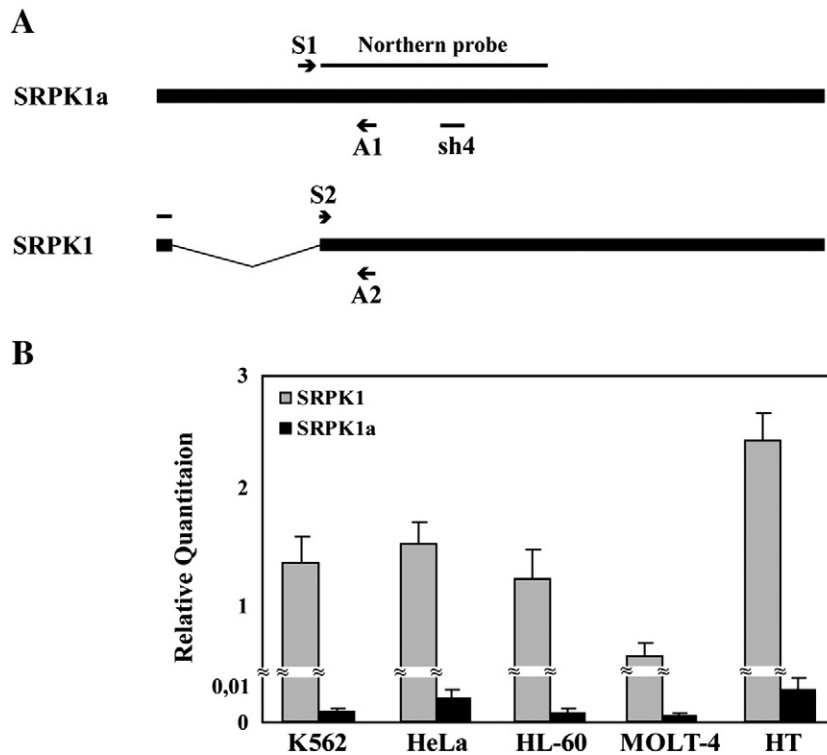


Fig. 1. Relative expression of SRPK1 and SRPK1a in various cancer cell lines. (A) Schematic representation of human SRPK1a and SRPK1. Arrows indicate the relative position of the primers used for Real Time PCR analysis (S1 and S2, sense primers; A1 and A2, antisense primers, see the respective sequences in Materials and methods). Bars indicate the target site of sh4-SRPK1 and the relative position of the probe used for Northern blotting analysis. (B) Relative quantitation of SRPK1 versus SRPK1a mRNA in testis and various cancer cell lines was assessed with the $2^{-\text{dCt}}$ method, based on equal efficiencies of the amplification protocols for both targets. A ready-made GUSB assay was used for normalization. Experiments were done in triplicate, bars denote standard deviation.

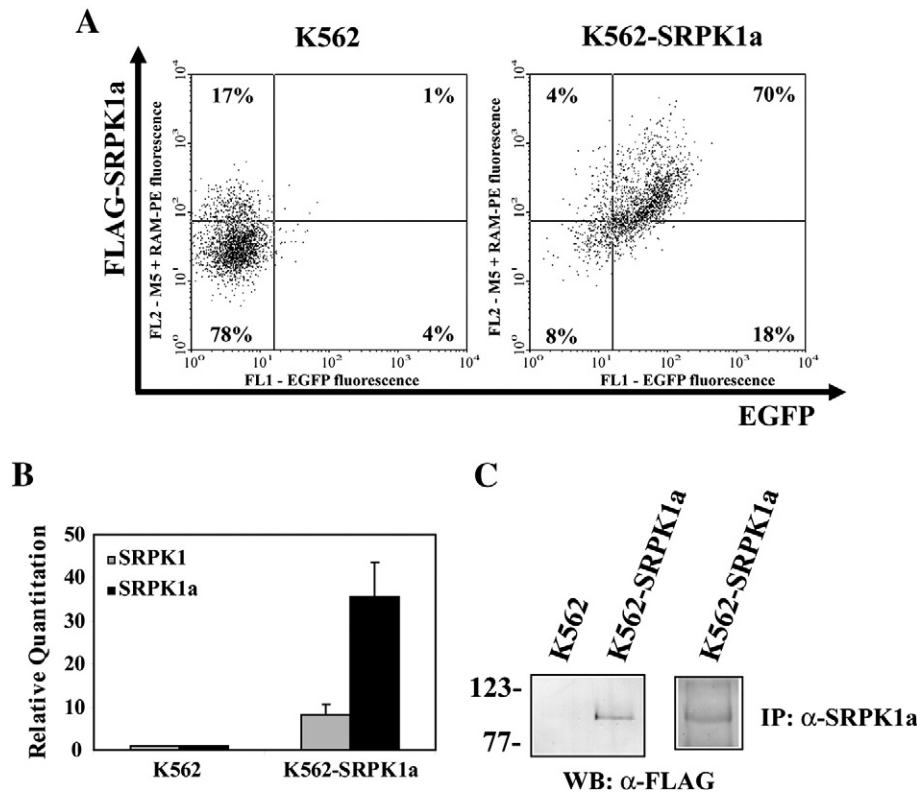


Fig. 2. Analysis of SRPK1a overexpression in K562 cells. (A) Flow cytometric intracellular detection of overexpressed FLAG-SRPK1a (Y axis) and EGFP (X axis) on parental K562 (left dot plot, negative control) and on genetically modified K562-SRPK1a cells (right dot plot). The majority of the parental cells were found in the lower left FLAG-SRPK1a(-)/EGFP(-) quadrant, whereas the majority of the K562-SRPK1a cells were found in the upper right FLAG-SRPK1a(+)/EGFP(+) quadrant. (B) Relative quantification of the mRNA of the two isoforms in K562-SRPK1a cells as compared to parental K562 cells were calculated using the $2^{-\Delta\Delta C_t}$ method. A ready-made *GUSB* assay was used for normalization. Experiments were done in triplicate, bars denote standard deviation. Black columns, SRPK1a; shaded columns, SRPK1. (C) Detection of overexpressed FLAG-SRPK1a in parental and K562-SRPK1a cells by immunoblotting analysis. Three hundred micrograms of lysates from parental and K562-SRPK1a cells, respectively, were analyzed on 10% SDS-polyacrylamide gels. The proteins were then transferred to nitrocellulose, and FLAG-SRPK1a was detected with the M5 anti-FLAG monoclonal antibody (left panel). In the right panel lysates from K562-SRPK1a cells were first immunoprecipitated with the anti-SRPK1a polyclonal antibody and the immunoprecipitate was subsequently immunoblotted with the anti-FLAG antibody.

analysis, followed by relative quantification of SRPK1 and SRPK1a with the $2^{-\Delta\Delta C_t}$ method, revealed a four-fold decrease of the SRPK1/SRPK1a transcript ratio in K562-SRPK1a cells as compared with parental K562 cells (Fig. 2B). Overexpression of SRPK1a also enhanced to some extent the expression of SRPK1 in K562-SRPK1a cells, most likely because part of the overexpressed SRPK1a underwent splicing.

The effects of SRPK1a overexpression in K562 cells were studied by monitoring proliferation and clonogenicity as well as by recording both cellular morphology and phenotype. The SRPK1a overexpressing cells were found to be notably growth-retarded as compared to their control counterparts (Fig. 3A). In addition, a significant amount of cells were smaller as compared to the parental K562 cells. Interestingly, the pellets of K562-SRPK1a cells were strikingly more red as compared to the parental cells, indicating the production of hemoglobin. The induced synthesis of hemoglobin was evident by staining the cells with a benzidine-peroxide solution (Fig. 3B) and also by SDS-PAGE analysis of cell extracts from parental and K562-SRPK1a cells, followed by Coomassie blue staining (Fig. 3C).

The outcome of SRPK1a overexpression in plating efficiency and growth of K562 cells was subsequently studied by clonogenic assays. In this respect, K562 and K562-SRPK1a cells were plated (1000 cells) in serum-free or serum-containing methylcellulose medium in 6-well plates in the presence or absence of 2 U/ml erythropoietin (EPO) (see Materials and methods). The cultures were microscopically scored for colony formation after 14 days. As shown in Fig. 3D, while EPO induced K562 cell proliferation in serum-free medium, cells overexpressing SRPK1a showed an extremely low proliferation potential under the same conditions. In the presence of serum, the growth potential of K562-SRPK1a cells was impaired to a lesser extent, with

the parental K562 cells being able to form 1.9 (in the absence of EPO) to 2.4 times (in the presence of EPO) more colonies as compared to K562-SRPK1a cells.

3.3. Decreased SRPK1 levels lead to erythroid differentiation of K562 cells

Small inhibitory RNAs targeting SRPK1 mRNA have been previously used with success to specifically reduce SRPK1 expression in various cell lines, such as MiaPaCa2, Panc1, MCF7 and MCF10A cells [27,31].

Transient transfection of one of these constructs, sh4-SRPK1 encoding a siRNA that targets nucleotides 648 to 665 of the human SRPK1 mRNA (NM_003137.3), into K562 cells substantially reduced SRPK1 expression as confirmed by Western blot analysis (Fig. 4A). No changes in SRPK1 levels were detected in cells transfected with scr-SRPK1 encoding a scrambled version of the sh4 sequence (Fig. 4A, first lane). In agreement with the Western blot analysis, immunoprecipitation experiments using the anti-SRPK1 polyclonal antibody (recognizing both isoforms), followed by activity assays showed that transfection of the siRNA-encoding construct resulted in 75% inhibition of SRPK1 activity in K562 cells (Fig. 4B). Yet, transfection of the same siRNA-encoding construct had a significantly weaker effect on SRPK1a activity as judged by immunoprecipitation experiments using the specific anti-SRPK1a polyclonal antibody followed by activity assays. This was surprising, since sh4-SRPK1 encodes a siRNA targeting a common sequence of SRPK1 and SRPK1a mRNAs, within their spacer domain. To further substantiate the rather specific knockdown effect of sh4-SRPK1 on SRPK1 we performed Real Time PCR analysis. Relative quantification of SRPK1

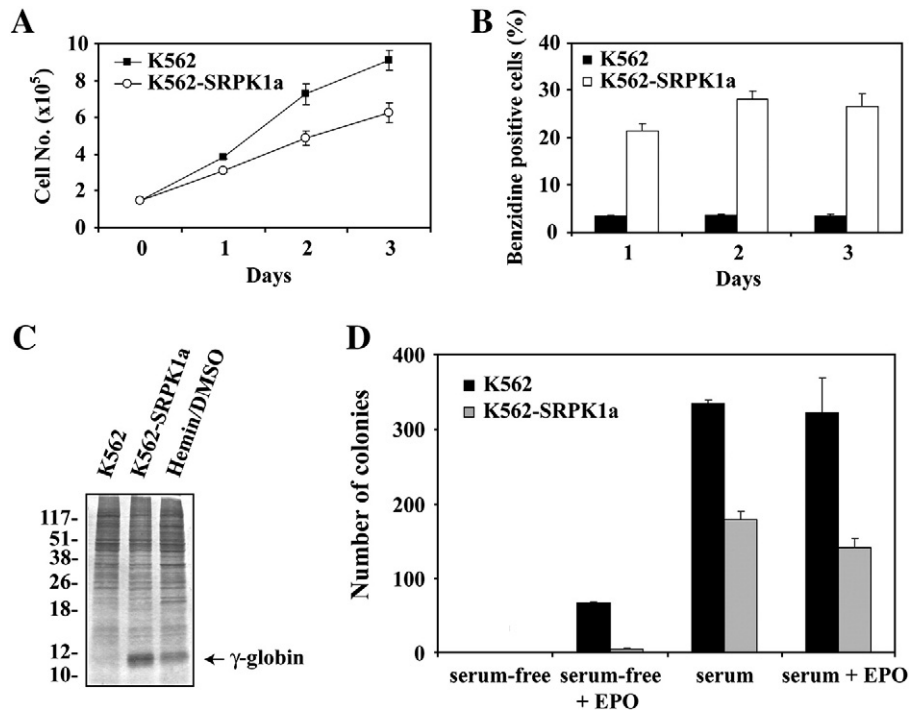


Fig. 3. Stable overexpression of SRPK1a promotes erythroid differentiation of K562 cells. (A) Growth rates of K562 and K562-SRPK1a cells. The total cell number was counted daily and represents the mean of four different experiments, bars denote standard deviation (for day 1, day 2 and day 3: $p < 0.01$ by Student t -test). (B) Exponentially growing K562 and K562-SRPK1a cells were seeded at 1×10^5 cells/ml and left to grow for 1, 2 and 3 days respectively. The percentage of benzidine-positive K562 (black columns) and K562-SRPK1a (shaded columns) cells was determined daily in order to quantify the proportion of hemoglobin-containing cells. The data reported represent the mean of three different experiments, bars denote standard deviation. (C) One hundred micrograms of cell extracts from control K562, K562-SRPK1a and hemin/DMSO-treated cells were analyzed on 12% SDS-polyacrylamide gels and then stained with Coomassie Brilliant Blue R-250. The arrow denotes the position of γ -globin. (D) K562-SRPK1a cells show reduced clonogenic potential. Parental and K562-SRPK1a cells were plated in serum-free or serum-containing methylcellulose medium in 6-well plates in the presence or absence of 2 U/ml EPO. A comparative presentation of the observed colonies number after 14 days of culture is shown. Black columns, K562 cells; shaded columns, K562-SRPK1a cells. All experiments were done in triplicate, bars denote standard deviation.

and SRPK1a with the 2^{-ddCt} method, in K562 cells electroporated with the sh4-SRPK1 plasmid as compared to cells electroporated with scr-SRPK1, revealed a decrease of the SRPK1/SRPK1a mRNA ratio ranging from 1.09 on the first day after transfection of sh4-SRPK1 to 3.25 and 3.01 on the fourth and fifth day after transfection respectively (Fig. 4C). The observed diminished inhibition of SRPK1a may be due to the fact that the extra segment of 513 bases at the 5' end drives SRPK1a mRNA to adopt a configuration that hinders the recognition of the targeted nucleotides by the siRNA.

K562 cells transiently transfected with sh4-SRPK1 exhibited a phenotype similar to K562-SRPK1a cells, in that they were smaller and their growth rate was significantly reduced as compared to control K562 cells (cells transiently transfected with scramble siRNA). Furthermore, cells transfected with sh4-SRPK1 were synthesizing significant amounts of hemoglobin as evidenced by staining the cells with a benzidine-peroxide solution (Fig. 4D) and also by SDS-PAGE analysis of cell extracts from K562 cells transfected with sh4-SRPK1 and scr-SRPK1, respectively, followed by Coomassie blue staining (Fig. 4E). It can therefore be concluded that a decreased SRPK1/SRPK1a ratio -arising either from down-regulating SRPK1 or overexpressing SRPK1a- leads to erythroid differentiation of K562 cells.

3.4. A decreased SRPK1/SRPK1a ratio is observed in K562 cells differentiated with hemin/DMSO and in human erythroid progenitor cells

If down-regulation of SRPK1 or alternatively overexpression of SRPK1a leads to erythroid differentiation of K562 cells, a similar decrease in SRPK1/SRPK1a ratio should also be observed in K562 cells induced to differentiate upon addition of hemin/DMSO. Indeed, as shown in Fig. 5A, Real Time PCR analysis of RNA samples extracted

from untreated K562 cells and cells incubated in the presence of 60 μ M hemin and 1.5% DMSO, followed by relative quantitation of SRPK1 and SRPK1a with the 2^{-ddCt} method, revealed an impressive decrease of the SRPK1/SRPK1a transcript ratio in hemin/DMSO-treated K562 cells as compared to the untreated cells. Notably, the observed decrease of the SRPK1/SRPK1a mRNA ratio was far more pronounced on the first day of differentiation (19.4-fold) and then dropped to 8.2-, 6.8- and 2.6-fold, on the second, third and fourth day, respectively, implying that it is closely related to the initial triggering of leukaemic cells to differentiate (Fig. 5A).

In addition, if SRPK1a is engaged in erythroid differentiation then human erythroid progenitor cells should also express relatively high levels of SRPK1a. In primary erythroid cells, SRPK1 was still the predominant isoform, yet the SRPK1/SRPK1a transcript ratio dropped dramatically to 27 as compared to the value of 480 observed in K562 leukaemic cells (Fig. 5B), further suggesting that the decreased SRPK1/SRPK1a ratio is probably associated with the commitment of primary cells to differentiate. In line with this hypothesis, terminal erythroid differentiation of the progenitor cells resulted in only a further minor decrease of the relative SRPK1/SRPK1a mRNA expression as compared to the untreated cells. (Fig. 5C).

3.5. Overexpressed SRPK1a localizes in the microsomal fraction, cytoplasm and nuclear matrix of K562-SRPK1a cells and does not affect SR protein phosphorylation

SR proteins that mediate both constitutive and alternative splicing of pre-mRNAs have been considered as the quintessential targets of SRPKs [3,6]. In addition, a BCR/ABL-dependent change in pre-mRNA processing together with an increase in SRPK1 expression were observed in p210BCR/ABL-eGFP-transduced umbilical cord blood

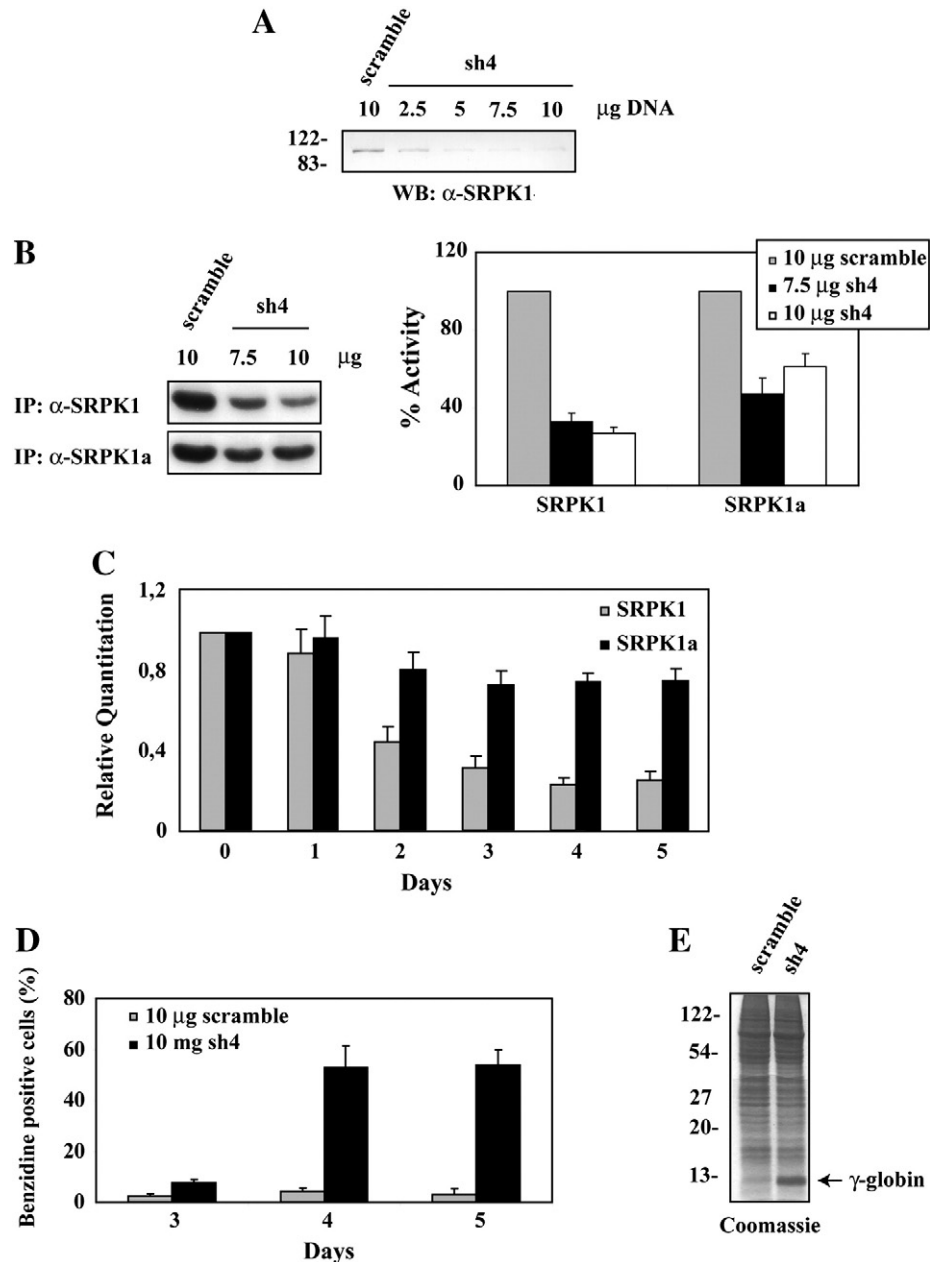


Fig. 4. Down-regulation of SRPK1 levels lead to erythroid differentiation of K562 cells. (A) K562 cells were transfected with either 2.5, 5, 7.5 and 10 µg of sh4-SRPK1 constructs or 10 µg of the scr-SRPK1 construct that encode a siRNA targeting the SRPK1 transcript or a scrambled version of this sequence, respectively. Western blot analysis was then performed on transfectants to determine their effects on the expression of SRPK1. (B) Immunoprecipitations from cell extracts derived from K562 cells transfected with scr-SRPK1 (10 µg) or sh4-SRPK1 (7.5 and 10 µg, respectively) were performed with an anti-SRPK1 polyclonal antibody (recognizing both isoforms) and a specific anti-SRPK1a polyclonal antibody and the immunoprecipitates were assayed for RS kinase activity, using the N-terminal domain of LBR fused to GST (GST-LBRNt) as substrate. The samples were analyzed by SDS-PAGE and autoradiographed. The bands corresponding to full-length labeled GST-LBRNt are shown (left panel). The radioactive bands were excised, and the radioactivity was determined by Cerenkov counting (right panel). Data are presented as % relative activity of sh4-SRPK1 transfected K562 cells. The activity of scr-SRPK1 transfected cells was set to be 100. Bars denote standard deviation. Shaded columns, scr-SRPK1 transfected; black columns, sh4-SRPK1 transfected (7.5 µg); open columns sh4-SRPK1 transfected (10 µg). (C) Relative quantitation of SRPK1/SRPK1a mRNA in K562 cells electroporated with the sh4-SRPK1 plasmid as compared to cells electroporated with scr-SRPK1 were calculated 1, 2, 3, 4 and 5 days after transfection using the 2^{-ddct} method. A ready-made *GUSB* assay was used for normalization. Experiments were performed in triplicate, bars denote standard deviation. Black columns, SRPK1a; shaded columns, SRPK1. (D) The percentage of benzidine-positive scr-SRPK1 transfected (shaded columns) and sh4-SRPK1 transfected K562 cells (black columns) were determined 3, 4 and 5 days after transfection in order to quantify the proportion of hemoglobin-containing cells. The data represent the mean of three different experiments, bars denote standard deviation. (E) One hundred micrograms of cell extracts from scr-SRPK1 (10 µg) and sh4-SRPK1 (10 µg) transfected cells were analyzed on 12% SDS-polyacrylamide gels and then stained with Coomassie Brilliant Blue R-250. The arrow denotes the position of γ -globin.

CD34+ cells [32]. To investigate the effect that overexpression of SRPK1a had upon SR protein phosphorylation, we performed Western blotting analysis on cell lysates produced from control and K562 cells overexpressing SRPK1a, using the mAb104 monoclonal antibody. mAb104 binds a conserved phosphoepitope on the family of SR proteins, consisting of the consecutive RS dipeptides [33]. As shown in Fig. 6 overexpressed SRPK1a did not enhance the level of SR protein

phosphorylation in K562-SRPK1a cells. On the contrary, a minor decrease in the intensity of a band with molecular mass of ~35 kDa and a more substantial reduction of a second band at 119 kDa were observed.

The lack of increased SR protein phosphorylation suggested that overexpressed SRPK1a may not be distributed in the nucleus of K562-SRPK1a cells. To examine the subcellular localization of FLAG-SRPK1a

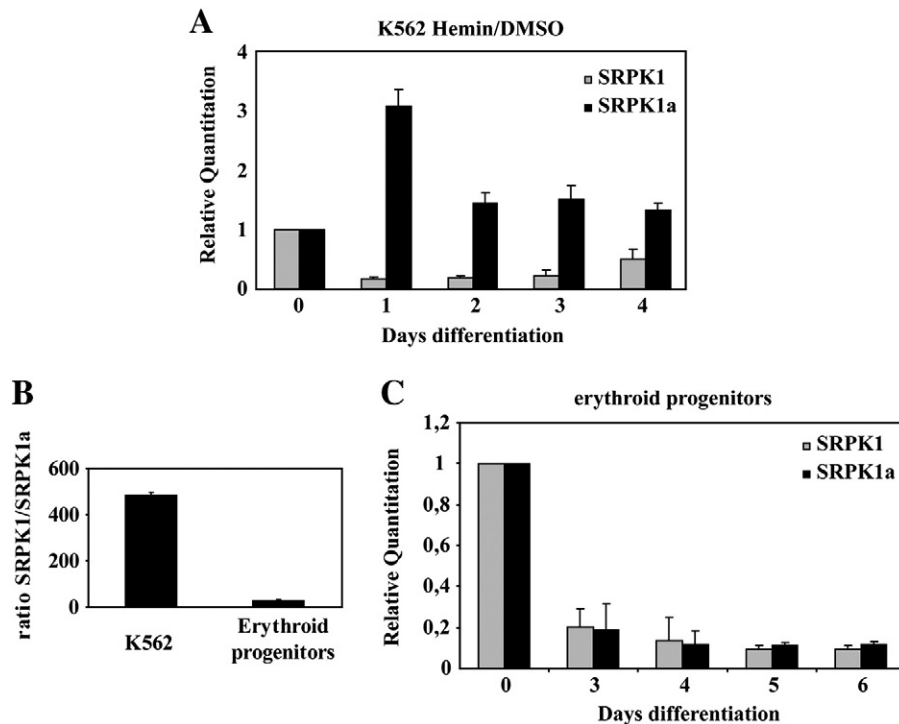


Fig. 5. A decreased SRPK1/SRPK1a ratio is observed in hemin/DMSO-treated K562 cells and in human erythroid progenitor cells. (A) Relative quantitation of SRPK1/SRPK1a mRNA in K562 cells treated with hemin/DMSO for 1, 2, 3 and 4 days, respectively, as compared to parental K562 cells (day 0 of differentiation) were calculated using the $2^{-\Delta\Delta Ct}$ method. A ready-made *GUSB* assay was used for normalization. Experiments were performed in triplicate, bars denote standard deviation. Black columns, SRPK1a; shaded columns, SRPK1. (B) Relative quantitation of SRPK1 versus SRPK1a mRNA in K562 and erythroid progenitor cells was assessed automatically with the $2^{-\Delta Ct}$ method, based on equal efficiencies of the amplification protocols for both targets. A ready-made *CSNK1D* assay was used for normalization. Experiments were performed in triplicate, bars denote standard deviation. (C) Relative quantitation of SRPK1/SRPK1a mRNA in primary erythroid cells induced to differentiate (see [Materials and methods](#)) for 3, 4, 5 and 6 days, respectively, as compared to untreated cells (day 0 of differentiation) were calculated using the $2^{-\Delta\Delta Ct}$ method. A ready-made assay *CSNK1D* was used for normalization. Experiments were performed in triplicate, bars denote standard deviation. Black columns, SRPK1a; shaded columns, SRPK1.

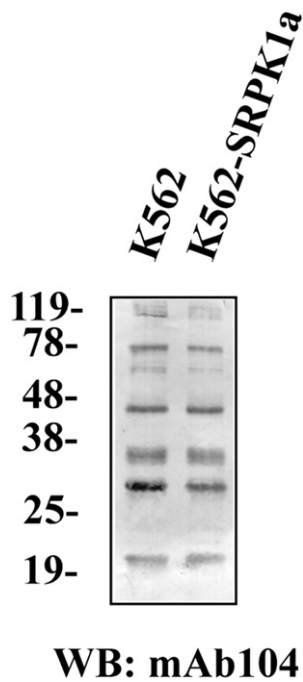


Fig. 6. Overexpression of SRPK1a does not impact SR protein phosphorylation. Three hundred micrograms of lysates from control and K562 cells overexpressing SRPK1a, respectively, were analyzed on 12% SDS-polyacrylamide gels. The proteins were then transferred to nitrocellulose, and phosphorylated SR proteins were detected with the mAb104 monoclonal antibody.

and also to compare it with the distribution of endogenous SRPKs in control cells we initially employed immunofluorescence microscopy. As shown in [Fig. 7A](#) (left panel), in parental K562 cells, SRPKs dispersed throughout the cell. Due to the large nuclei in K562 cells, there is little cellular space corresponding to the cytoplasm, thereby hampering definitive conclusions by immunofluorescence microscopy. In this respect we next employed biochemical fractionation methods. Briefly, the cell lysate was centrifuged at 4300g at 4 °C for 10 min to yield a supernatant (S1) and a crude nuclear fraction. This initial supernatant was further fractionated into cytoplasmic (S100) and microsomal (P100) fractions by centrifuging at 100,000g for 60 min at 4 °C. Purified nuclei were isolated by passing the crude nuclear fraction through a sucrose cushion and subjected to sequential extraction steps with high salt and DNaseI. The residual insoluble pellet was designated as the nuclear matrix fraction. Western blotting analysis of the different fractions obtained, using an anti-SRPK1 mouse monoclonal antibody that recognizes both isoforms, showed a single immunoreactive band, at ~97 kDa (probably corresponding to SRPK1 due to the very low levels of SRPK1a), in the S1 and nuclear fractions at roughly equivalent amounts ([Fig. 7A](#), right panel). The immunoreactive band detected in the S1 fraction upon further fractionation was analyzed in two bands, one associated with the cytoplasmic fraction (S100) and a stronger one associated with the P100 fraction ([Fig. 7A](#), right panel).

K562-SRPK1a cells exhibited a clearly different fluorescence pattern of total SRPKs (both endogenous and overexpressed), in that a discernible extranuclear localization was observed, with the nuclear staining being significantly weaker as compared to the parental cells (compare [Fig. 7B](#), left panel with [Fig. 7A](#), left panel). The peripheral rim fluorescence pattern was predominant when

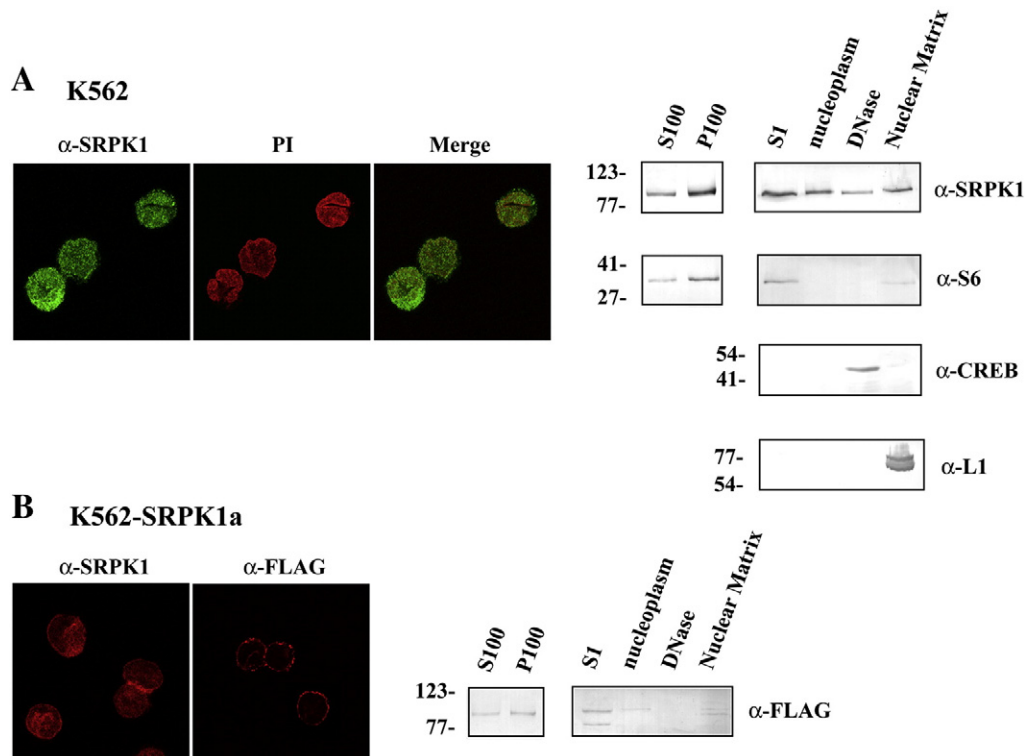


Fig. 7. Localization of endogenous SRPKs and FLAG-SRPK1a in control and K562-SRPK1a cells. (A) Fluorescence pattern of SRPKs in parental K562 cells (left panel). SRPKs were detected using the mouse monoclonal anti-SRPK1 antibody (FITC, green), while nuclei were stained with propidium iodide (PI). A dispersion of SRPKs throughout the entire cell is clearly seen. The distribution of SRPKs between different subcellular compartments was analyzed by immunoblotting using the monoclonal anti-SRPK1 antibody (right panel). Cell fractionation was performed as described in [Materials and methods](#). The distribution of CREB, lamins, and S6 ribosomal protein was used as a marker to test the purity of the individual compartments. A mouse monoclonal α -CREB, a polyclonal anti-lamin (α -L1) and a polyclonal α -S6 antibody were used for immunoblotting. (B) Fluorescence pattern of total SRPKs (both endogenous and overexpressed, left panel) and FLAG-SRPK1a (middle panel) in K562-SRPK1a cells. SRPKs were detected using the monoclonal anti-SRPK1 antibody (TRITC, red), while overexpressed FLAG-SRPK1a was detected using the specific anti-FLAG monoclonal antibody (TRITC, red). SRPKs localized in the nucleus, while a peripheral rim distribution pattern, was also seen. The peripheral, cytoplasmic distribution became predominant when cells were stained with anti-FLAG antibody, with a rather minor fraction seen in the nucleus. The distribution of FLAG-SRPK1a was also analyzed by immunoblotting, following biochemical fractionation, using the anti-FLAG antibody (right panel).

K562-SRPK1a cells were stained with the M5 anti-FLAG monoclonal antibody, while a rather weak speckled pattern was also seen in the nucleus ([Fig. 7B](#), middle panel). Biochemical fractionation methods confirmed the immunofluorescence data. Western blotting analysis, using the anti-FLAG monoclonal antibody, showed a strong immunoreactive band in the S1 fraction, which, similarly to the control cells, upon further fractionation was distributed between the P100 and S100 fractions, and a weaker one in the nuclear matrix fraction ([Fig. 7B](#), right panel). These data clearly demonstrate that overexpressed SRPK1a mainly localized in the microsomal fraction and the cytoplasm, and to a lesser extent in the nuclear matrix.

3.6. Purification and characterization of SRPK1a-associated complexes

In an attempt to identify proteins specifically associated with SRPK1a, we immunopurified FLAG-tagged SRPK1a from extracts of stably transfected K562 cells and identified the co-purified proteins by MS/MS based mass spectroscopy ([Fig. 8](#)). The known functions of these proteins as well as their subcellular localization, as extracted from the NCBI database, are listed in [Table 1](#). More detailed data on molecular weight, accession No, peptide hit number and the amino acid sequence of identified peptides of the SRPK1a-interacting proteins are provided in [Supplementary Table 1](#). Almost the entirety of the identified proteins were RNA-binding proteins localized both in the nucleus and the cytoplasm. Numerous RNA helicases, heterogeneous nuclear ribonucleoproteins, ribosomal proteins, and mRNA-associated proteins were found and among them several had been previously identified in ribosomal and pre-ribosomal complexes. As listed in [Table 2](#), of the twenty-one proteins identified in our SRPK1a

complex, nine were previously identified as components of the human Nop56p-associated pre-ribosomal RNP complex involved in ribosome biogenesis [34], nine were found associated with the nucleolin protein complex that may be actively involved in ribosome biogenesis and maturation [35], three were found associated with the

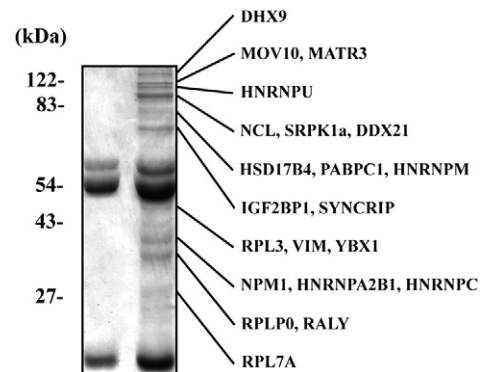


Fig. 8. Isolation and characterization of SRPK1a-associated proteins. SRPK1a-associated complexes were isolated by immunoprecipitation of FLAG-SRPK1a from K562-SRPK1a cells with the anti-FLAG monoclonal antibody. Before immunoprecipitation the cell lysate was precleared by incubating with protein A-Sepharose. Immunoprecipitates were analyzed by SDS-PAGE on a 12.5% gel followed by Coomassie blue staining. Lane 1, protein bands derived from the anti-FLAG monoclonal antibody; lane 2, proteins co-immunoprecipitated with FLAG-SRPK1a. Specific bands were excised from the gel, subjected to in-gel protease digestion and analyzed by reversed-phase LC-MS/MS. The resulting peptide fragment fingerprints were matched against a human protein sequence database. Gel bands are annotated with the identity of the proteins found in the corresponding in-gel digests. Bars on the left indicate molecular masses (in kDa).

Table 1

Components of the SRPK1a protein complex. The known functions of proteins in humans and their subcellular localization were extracted from the NCBI database.

Protein	Known function in humans	Subcellular localization
DHX9	DEAH (Asp-Glu-Ala-His) box polypeptide 9, ATP-dependent RNA helicase	cytoplasm, nucleus
MOV10	Moloney leukaemia virus 10 homolog, putative RNA helicase	cytoplasm
MATR3	matrin 3, associated with the nuclear matrix, unknown function	nucleus
HNRNPU (SAF-A)	pre-mRNA processing, mRNA metabolism and transport, binds scaffold-attachment regions of genomic DNA	nucleus
Nucleolin	nucleolar phosphoprotein, involved in the synthesis and maturation of ribosomes	nucleus, cell cortex
SRPK1a	Serine/Arginine Protein Kinase 1a, phosphorylates RS domains	cytoplasm, nucleus
DDX21	DEAD (Asp-Glu-Ala-Asp) box polypeptide 21, RNA helicase	nucleus
HSD17B4	hydroxysteroid (17- β) dehydrogenase 4, involved in the peroxisomal beta-oxidation pathway for fatty acids	mitochondrion, peroxisome
PABPC1	poly(A) binding protein, required for poly(A) shortening and translation initiation	cytoplasm, nucleus
HNRNPM	pre-mRNA processing, mRNA metabolism and transport	nucleus
IGF2BP1	insulin-like growth factor 2 mRNA binding protein 1, binds to and regulates the translation of mRNAs	cytoplasm, nucleus
SYNCRIP	synaptotagmin binding, cytoplasmic RNA interacting protein	cytoplasm, nucleus, microsome
RPL3	60 S ribosomal protein L3, structural constituent of ribosome	cytoplasm, nucleus, ribosome
Vimentin	intermediate filament protein, maintaining cell shape, cytoplasmic integrity, and cytoskeletal interactions	cytoplasm, cytoskeleton
YBX1	Y box binding protein 1, binds RNA, dsDNA, ssDNA, functions as a transcriptional regulator	cytoplasm, nucleus
Nucleophosmin (NPM1)	ribosomal protein assembly and transport, control of centrosome duplication, regulation of ARF	cytoplasm, nucleus
HNRNPA2B1	pre-mRNA processing, mRNA metabolism and transport	cytoplasm, nucleus
HNRNPC	pre-mRNA processing, mRNA metabolism and transport	nucleus
RPLP0	60 S acidic ribosomal protein P0, structural constituent of ribosome	cytoplasm, ribosome
RPL7A	60 S ribosomal protein L7A, structural constituent of ribosome	cytoplasm, ribosome
RALY	RNA binding protein, autoantigenic (hnRNP-associated with lethal yellow homolog (mouse))	nucleus

nucleophosmin protein complex that was recently shown to mediate nuclear export of mammalian ribosomes [36] and three were identified as components of the large Drosha complex that was proposed to mediate preribosomal RNA processing ([37,38], see also Biomolecular Interaction Network Database). Furthermore, five proteins of the SRPK1a complex were previously identified to be part of a complex that regulates c-myc mRNA stability [39]. Interestingly, DHX9 helicase, HNRNPU (SAF-A), nucleolin, HNRNPM, YBX1 and nucleophosmin were identified in at least three of the above complexes, while SRPK1a itself has been reported to be a component of both the Nop56p and large Drosha complexes (Table 2), demonstrating the effectiveness of our proteomic approach.

Although we have been unable to identify the actual substrates of SRPK1a, since none of the SRPK1a-associated proteins contained an RS domain and therefore could not be directly phosphorylated by the kinase, our data point to the conclusion that SRPK1a is associated with ribosome assembly and function and furthermore that it is via this

Table 2

Previously identified protein complexes containing components of the SRPK1a protein complex Nop56p: Nop56p-associated pre-ribosomal ribonucleoprotein complex involved in ribosome biogenesis [34]; NucPC: Nucleolin Protein Complex, that might be involved in ribosome biogenesis and maturation [35]; NPC: Nucleophosmin Protein Complex that mediates nuclear export of mammalian ribosome [36]; LMC: Large Microprocessor Complex that mediates the genesis of miRNAs and might also mediate preribosomal RNA processing [37,38]; myc: complex that controls c-myc mRNA stability [39].

	Nop56p	NucPC	NPC	LMC	myc
DHX9	+	+	+		+
MOV10					
MATR3					
HNRNPU (SAF-A)	+	+		+	+
Nucleolin	+	+	+		
SRPK1a	+			+	
DDX21	+				
HSD17B4					
PABPC1					
HNRNPM	+	+			
IGF2BP1	+				+
SYNCRIP					+
RPL3		+			
Vimentin					
YBX1	+	+			+
Nucleophosmin (NPM1)	+	+	+		
HNRNPA2B1					
HNRNPC					
RPLP0		+			
RPL7A		+			
RALY				+	

particular function that SRPK1a promotes erythroid differentiation in K562 cells.

4. Discussion

SRPK1a has been cloned in 2001 [2] but has received minimal attention up to now. SRPK1a escaped notice because of its very low expression levels and difficult detection. The extra segment of SRPK1a shows a loop structure at the RNA level, with extended double-stranded domains (<http://rna.tbi.univie.ac.at/cgi-bin/RNAfold.cgi>; E. Nikolakaki, unpublished observations) resulting in poor detection by Northern and RT-PCRs. In this respect, and after several tests, we found that only when using sense primers from the 3' region of intron I (spliced out in SRPK1), very close to the common sequence (see Materials and methods), we observe efficient amplification. Furthermore, the antigenicity of the extended N-terminal domain of the protein is very low, rendering all our efforts to raise specific peptide antibodies unsuccessful. The only available antibody so far was raised against the whole N-terminal domain of SRPK1a fused to GST and is functional only in immunoprecipitations.

A variety of roles and functions have been attributed exclusively to SRPK1, while the contribution of SRPK1a to these diverse functions remains largely unknown. In the present study, using K562 cells as a model system, we found that the ratio of SRPK1 to SRPK1a is critical in determining K562 cell fate, with SRPK1 favouring proliferation and SRPK1a favouring differentiation. Our data are in line with previous reports indicating that SRPK1 levels were up-regulated in pancreatic, breast and colonic tumors where its expression increased coordinately with tumor grade [27,31]. Furthermore, it was shown that high levels of expression of SRPK1 were associated with resistance of various cell lines to chemotherapeutic agents such as oxaliplatin, gemcitabine and cisplatin [27,31,40].

An important issue arising from these findings are the functional differences between SRPK1 and SRPK1a that might account for the association of high SRPK1 levels with proliferation in contrast to the reduction in proliferation and induction of erythroid differentiation followed by stable SRPK1a overexpression in K562 cells. Except for the

fact that SRPK1a is 3- to 4-fold more active than SRPK1, both isoforms exhibit the same specificity, as judged by their ability to phosphorylate various derivatives of the NH₂-terminal domain of LBR, in which one or more serines of the RS domain were mutated to Gly or Ala [2]. Furthermore, both SRPK1 and SRPK1a were able to induce alternative splicing of human tau exon 10 in transfected cells [2], while, as shown in the present study, overexpression of SRPK1a had no significant effect upon SR protein phosphorylation. Differential localization and the consequent targeting of specific substrates might therefore be the reason for their distinct cellular functions. SRPK1 distributed almost equally between the nucleus and the extranuclear space of control K562 cells, whereas only a small amount of SRPK1a exhibited nuclear localization, and was associated with the nuclear matrix. It is therefore possible that the nuclear localization of SRPK1 accounts for its implication in several key events related to the proliferation potential of human leukaemic cells. These key events may or may not relate to phosphorylation regulation of pre-mRNA processing. In this respect, SRPK1 may phosphorylate substrates that are not related to pre-mRNA splicing, such as LBR, thereby regulating the attachment of chromatin to the nuclear periphery [16,17] and/or other yet unidentified substrates.

Interestingly, the majority of SRPK1a was found associated with the microsomal (P100) fraction, while a considerable amount of extranuclear SRPK1 was also found associated with the same fraction. Whether the microsomal association of SRPKs in K562 cells is cell type-specific or represents a more general localization pattern, applicable to other cell lines as well, remains at present unknown and represents an interesting subject for future studies. In keeping with the latter possibility, Wang et al. reported that both SRPK1 and SRPK2 were found to localize in the cytoplasm of adherent cells but in a nondiffused fashion, with the underlying cytoplasmic structure remaining to be characterized [5]. Furthermore, the predominant association of SRPK1a with the P100 fraction, but also its presence at the nuclear matrix (the nucleolus, where ribosome biogenesis gets under way, is considered as being part of the nuclear matrix) corroborates well with the data from mass spectrometric analysis of immunopurified SRPK1a-associated complexes. SRPK1a complexes were shown to contain a variety of RNA-binding proteins, such as RNA helicases, heterogeneous nuclear ribonucleoproteins, ribosomal proteins, and mRNA-associated proteins, the majority of which are known players in ribosome processing and function, and have been previously identified in ribosomal and pre-ribosomal complexes. It is therefore possible that SRPK1a mainly -but SRPK1 as well to some extent- may be associated with polysomes. Preliminary data confirm that SRPK1a associates with ribosomes in K562-SRPK1a cells, thereby suggesting that the kinase may have an active role in ribosome function and/or structure (data not shown).

An important question is whether the observed interactions are specific for SRPK1a. In this regard it should be pointed out that despite our efforts we have been so far unable to generate a K562 cell line overexpressing SRPK1, while even transient overexpression of SRPK1 in K562 cells was inefficient. Preliminary proteomic analysis of the SRPK1-associated proteins in control K562 cells revealed that some of the proteins found associated with SRPK1a bind also to SRPK1 (IGF2BP1, SYNCRIP, HNRNPA2B1 and HNRNPC), whereas others not (data not shown). We have not detected any of the proteins previously identified to be part of the Nop56 and the large Droscha complexes. The association of these proteins seem to be more specific, taking also into consideration that the proteomic analyses performed by the groups who characterized the large Droscha and the Nop56 complexes lead to the identification exclusively of SRPK1a and not of both isoforms [34,37].

Several reports document a link between ribosomal function and erythroid differentiation in human leukaemic cells. First, mutations in several ribosomal proteins lead to Diamond-Blackfan anemia, a syndrome characterized by defective erythropoiesis, congenital

anomalies, and increased frequency of cancer [41]. Second, when K562 cells were induced to differentiate by dimethyl sulfoxide and hemin, the observed differentiation was accompanied by a rapid increase in the rRNA levels [42]. In a similar study, activation of ribosomal gene clusters has been observed in hemin-induced K562 cells, 48 h after hemin induction [43]. Third, erythroid precursor cells, a primitive cell population which precedes the appearance of definitive erythroid elements, and early erythroid cells were shown to be engaged mainly in ribosomal production, including synthesis of rRNA and ribosomal proteins [44].

Unluckily, the specific substrates targeted by SRPK1a remain unknown at present, since none of the SRPK1a-associated proteins identified by mass spectrometric analysis was found to contain an RS domain. The lack of these critical data make difficult to directly address the question of how SRPK1a mediates differentiation of K562-SRPK1a cells. An interesting hint that could potentially link the SRPK1a partners with ribosomal assembly and protein synthesis as well as with the transcription of specific genes that are critical to differentiation is the observation that five proteins of the SRPK1a complex were previously implicated in regulating c-myc mRNA stability [39]. c-myc seems to play a critical role in coordinating protein synthesis through the transcriptional control of RNA and protein components of ribosomes, and also of gene products required for the processing of ribosomal RNA, the nuclear export of ribosomal subunits and the initiation of mRNA translation [45]. Yet, when we tested the c-myc mRNA levels by Real-Time PCR in control and K562-SRPK1a cells we were unable to detect any significant difference (data not shown). It is possible that the particular SRPK1a partners (DHX9, HNRNPU, IGF2BP1, SYNCRIP and YBX1) may also regulate the stability and/or translation of mRNA of other yet unknown regulatory proteins involved in ribosomal assembly and function.

At this point it should be also noted that numerous proteins originally thought to reside solely in the nucleolus, which is considered as the “ribosome factory,” have been shown to continuously shuttle from the nucleolus to various subcellular compartments in a regulated manner ([36] and references therein) and exert diverse functions. A typical example is nucleophosmin, a common component of the nucleophosmin protein complex [36], the nucleolin protein complex [35], the Nop56p-associated ribonucleoprotein complex [34], and the SRPK1a complex. In line with its participation in all the above protein complexes, nucleophosmin -besides residing in the nucleolus- has been found in several other subnuclear destinations [46–48] and was also shown to shuttle from the nucleus to the cytoplasm in a CRM1-dependent manner [49]. Furthermore, besides its well-documented role in ribosome biogenesis, nucleophosmin was shown to regulate transcription [50], while in a certain type of chronic lymphocytic leukaemia (CLL) it was highly expressed in the cytoplasm and was found associated with ribosomes [51]. A second example is nucleolin, identified in the same protein complexes as nucleophosmin. Nucleolin is found in various cell compartments, ranging from the nucleolus, of which it is a major component, to the cell surface [52]. Besides mediating the processing of ribosomal RNA, nucleolin may function as a histone chaperone and a chromatin co-remodeler, thereby regulating transcription. Furthermore, nucleolin was found associated with CD154 mRNA (coding for a protein which is critical in mediating immune responses) in both the ribonucleoprotein and polysome fractions and is involved in the regulation of its rate of turnover [53].

The identification of the specific substrates of SRPK1a and the delineation of how does this kinase with its associated proteins mediate erythroid differentiation form the basis of the upcoming studies. These studies not only will help deciphering the potential involvement of SRPK1a in ribosome assembly and function but more importantly will provide valuable insights on the molecular machinery that directs erythroid differentiation in human leukaemic cells.

Supplementary materials related to this article can be found online at doi:10.1016/j.bbamcr.2010.07.008.

Acknowledgments

We thank J. Tazi and S. Georgatos for the mAb104 monoclonal and the α -L1 polyclonal antibodies respectively. We also thank T. Giannakouros and J. G. Georgatsos for valuable discussions and comments on the manuscript. Morphological work was performed at the Confocal and Video Microscopy Unit of the University of Ioannina. This work was supported in part by grants from the Empirikon Foundation and the Greek Ministry of Education (PYTHAGORAS II No 80913) to E. Nikolakaki. A. Kolbus and M. Mairhofer are supported by a grant from the European Union (LSHB-CT-2006-037261). I. Sanidas was a recipient of a fellowship from the Greek State Scholarship's Foundation (I.K.Y.). P. Ponsaerts holds a postdoctoral fellowship of the Fund for Scientific Research-Flanders (FWO-Vlaanderen).

References

- [1] O. Nakagawa, M. Arnold, M. Nakagawa, H. Hamada, J.M. Shelton, H. Kusano, T.M. Harris, G. Childs, K.P. Campbell, J.A. Richardson, I. Nishino, E.N. Olson, Centronuclear myopathy in mice lacking a novel muscle-specific protein kinase transcriptionally regulated by MEF2, *Genes Dev.* 19 (2005) 2066–2077.
- [2] E. Nikolakaki, R. Kohen, A.M. Hartmann, S. Stamm, E. Georgatsou, T. Giannakouros, Cloning and characterization of an alternatively spliced form of SR protein kinase 1 that interacts specifically with scaffold attachment factor-B, *J. Biol. Chem.* 276 (2001) 40175–40182.
- [3] H.Y. Wang, K.C. Arden, J.R. Bermingham Jr., C.S. Viars, W. Lin, A.D. Boyer, X.D. Fu, Localization of serine kinases, SRPK1 (SFRSK1) and SRPK2 (SFRSK2), specific for the SR family of splicing factors in mouse and human chromosomes, *Genomics* 57 (1999) 310–315.
- [4] S. Papoutsopoulou, E. Nikolakaki, G. Chalepakis, V. Kruff, P. Chevillier, T. Giannakouros, SR protein-specific kinase 1 is highly expressed in testis and phosphorylates protamine 1, *Nucleic Acids Res.* 27 (1999) 2972–2980.
- [5] H.Y. Wang, W. Lin, J.A. Dyck, J.M. Yeakley, Z. Songyang, L.C. Cantley, X.D. Fu, SRPK2: a differentially expressed SR protein-specific kinase involved in mediating the interaction and localization of pre-mRNA splicing factors in mammalian cells, *J. Cell Biol.* 140 (1998) 737–750.
- [6] J.F. Gui, W.S. Lane, X.D. Fu, A serine kinase regulates intracellular localization of splicing factors in the cell cycle, *Nature* 369 (1994) 678–682.
- [7] J.F. Gui, H. Tronchere, S.D. Chandler, X.D. Fu, Purification and characterization of a kinase specific for the serine- and arginine-rich pre-mRNA splicing factors, *Proc. Natl. Acad. Sci. USA* 91 (1994) 10824–10828.
- [8] E. Nikolakaki, G. Simos, S.D. Georgatos, T. Giannakouros, A nuclear envelope-associated kinase phosphorylates arginine-serine motifs and modulates interactions between the lamin B receptor and other nuclear proteins, *J. Biol. Chem.* 271 (1996) 8365–8372.
- [9] T. Misteli, J.F. Caceres, D.L. Spector, The dynamics of a pre-mRNA splicing factor in living cells, *Nature* 387 (1997) 523–527.
- [10] T. Misteli, D.L. Spector, RNA polymerase II targets pre-mRNA splicing factors to transcription sites in vivo, *Mol. Cell* 3 (1999) 697–705.
- [11] J.E. Mermoud, P.T. Cohen, A.I. Lamond, Regulation of mammalian spliceosome assembly by a protein phosphorylation mechanism, *EMBO J.* 13 (1994) 5679–5688.
- [12] W. Gilbert, C. Guthrie, The Glc7p nuclear phosphatase promotes mRNA export by facilitating association of Mex67p with mRNA, *Mol. Cell* 13 (2004) 201–212.
- [13] M.C. Lai, R.I. Lin, W.Y. Tarn, Transportin-SR2 mediates nuclear import of phosphorylated SR proteins, *Proc. Natl. Acad. Sci. USA* 98 (2001) 10154–10159.
- [14] H. Polioudaki, N. Kourmouli, V. Drosou, A. Bakou, P.A. Theodoropoulos, P.B. Singh, T. Giannakouros, S.D. Georgatos, Histones H3/H4 form a tight complex with the inner nuclear membrane protein LBR and heterochromatin protein 1, *EMBO Rep.* 2 (2001) 920–925.
- [15] Q. Ye, H.J. Worman, Primary structure analysis and lamin B and DNA binding of human LBR, an integral protein of the nuclear envelope inner membrane, *J. Biol. Chem.* 269 (1994) 11306–11311.
- [16] M. Takano, Y. Koyama, H. Ito, S. Hoshino, H. Onogi, M. Hagiwara, K. Furukawa, T. Horigome, Regulation of binding of lamin B receptor to chromatin by SR protein kinase and cdc2 kinase in *Xenopus* egg extracts, *J. Biol. Chem.* 279 (2004) 13265–13271.
- [17] M. Takano, M. Takeuchi, H. Ito, K. Furukawa, K. Sugimoto, S. Omata, T. Horigome, The binding of lamin B receptor to chromatin is regulated by phosphorylation in the RS region, *Eur. J. Biochem.* 269 (2002) 943–953.
- [18] I. Mylonis, V. Drosou, S. Brancorsini, E. Nikolakaki, P. Sassone-Corsi, T. Giannakouros, Temporal association of protamine 1 with the inner nuclear membrane protein lamin B receptor during spermiogenesis, *J. Biol. Chem.* 279 (2004) 11626–11631.
- [19] K. Poplonska, M. Kwiatkowska, A. Wojtczak, J. Polit, Immunogold evidence suggests that endoplasmic reticulum is the site of protamine-type protein synthesis and participates in translocation of these proteins into the nucleus during *Chara vulgaris* spermiogenesis, *Biol. Reprod.* 80 (2009) 572–580.
- [20] J.H. Ding, X.Y. Zhong, J.C. Hagopian, M.M. Cruz, G. Ghosh, J. Feramisco, J.A. Adams, X.D. Fu, Regulated cellular partitioning of SR protein-specific kinases in mammalian cells, *Mol. Biol. Cell* 17 (2006) 876–885.
- [21] J. Koizumi, Y. Okamoto, H. Onogi, A. Mayeda, A.R. Krainer, M. Hagiwara, The subcellular localization of SF2/ASF is regulated by direct interaction with SR protein kinases (SRPKs), *J. Biol. Chem.* 274 (1999) 11125–11131.
- [22] X.Y. Zhong, J.H. Ding, J.A. Adams, G. Ghosh, X.D. Fu, Regulation of SR protein phosphorylation and alternative splicing by modulating kinetic interactions of SRPK1 with molecular chaperones, *Genes Dev.* 23 (2009) 482–495.
- [23] M. Takeuchi, M. Yanagida, A mitotic role for a novel fission yeast protein kinase *dsk1* with cell cycle stage dependent phosphorylation and localization, *Mol. Biol. Cell* 4 (1993) 247–260.
- [24] N. Bianchi, C. Chiarabelli, M. Borgatti, C. Mischiati, E. Fibach, R. Gambari, Accumulation of gamma-globin mRNA and induction of erythroid differentiation after treatment of human leukaemic K562 cells with tallimustine, *Br. J. Haematol.* 113 (2001) 951–961.
- [25] H. Dolznig, A. Kolbus, C. Leberbauer, U. Schmidt, E.M. Deiner, E.W. Mullner, H. Beug, Expansion and differentiation of immature mouse and human hematopoietic progenitors, *Methods Mol. Med.* 105 (2005) 323–344.
- [26] H.W. Snoeck, S. Weekx, A. Mouljin, F. Lardon, M. Lenjou, G. Nys, P.C. Van Ranst, D.R. Van Bockstaele, Z.N. Berneman, Tumor necrosis factor alpha is a potent synergistic factor for the proliferation of primitive human hematopoietic progenitor cells and induces resistance to transforming growth factor beta but not to interferon gamma, *J. Exp. Med.* 183 (1996) 705–710.
- [27] G.M. Hayes, P.E. Carrigan, A.M. Beck, L.J. Miller, Targeting the RNA splicing machinery as a novel treatment strategy for pancreatic carcinoma, *Cancer Res.* 66 (2006) 3819–3827.
- [28] C. Maison, H. Horstmann, S.D. Georgatos, Regulated docking of nuclear membrane vesicles to vimentin filaments during mitosis, *J. Cell Biol.* 123 (1993) 1491–1505.
- [29] M. Jiang, T. Axe, R. Holgate, C.P. Rubbi, A.L. Okorokov, T. Mee, J. Milner, p53 binds the nuclear matrix in normal cells: binding involves the proline-rich domain of p53 and increases following genotoxic stress, *Oncogene* 20 (2001) 5449–5458.
- [30] V. Kruff, H. Eubel, L. Jansch, W. Werhahn, H.P. Braun, Proteomic approach to identify novel mitochondrial proteins in *Arabidopsis*, *Plant Physiol.* 127 (2001) 1694–1710.
- [31] G.M. Hayes, P.E. Carrigan, L.J. Miller, Serine-arginine protein kinase 1 over-expression is associated with tumorigenic imbalance in mitogen-activated protein kinase pathways in breast, colonic, and pancreatic carcinomas, *Cancer Res.* 67 (2007) 2072–2080.
- [32] S. Salesses, S.J. Dylla, C.M. Verfaillie, p210BCR/ABL-induced alteration of pre-mRNA splicing in primary human CD34+ hematopoietic progenitor cells, *Leukemia* 18 (2004) 727–733.
- [33] A.M. Zahler, W.S. Lane, J.A. Stolk, M.B. Roth, SR proteins: a conserved family of pre-mRNA splicing factors, *Genes Dev.* 6 (1992) 837–847.
- [34] T. Hayano, M. Yanagida, Y. Yamauchi, T. Shinkawa, T. Isobe, N. Takahashi, Proteomic analysis of human Nop56p-associated pre-ribosomal ribonucleoprotein complexes. Possible link between Nop56p and the nucleolar protein treacle responsible for Treacher Collins syndrome, *J. Biol. Chem.* 278 (2003) 34309–34319.
- [35] M. Yanagida, A. Shimamoto, K. Nishikawa, Y. Furuichi, T. Isobe, N. Takahashi, Isolation and proteomic characterization of the major proteins of the nucleolin-binding ribonucleoprotein complexes, *Proteomics* 1 (2001) 1390–1404.
- [36] L.B. Maggi Jr., M. Kuchenruether, D.Y. Dadey, R.M. Schwoppe, S. Grisendi, R.R. Townsend, P.P. Pandolfi, J.D. Weber, Nucleophosmin serves as a rate-limiting nuclear export chaperone for the mammalian ribosome, *Mol. Cell Biol.* 28 (2008) 7050–7065.
- [37] R.I. Gregory, K.P. Yan, G. Amuthan, T. Chendrimada, B. Doratotaj, N. Cooch, R. Shiekhattar, The Microprocessor complex mediates the genesis of microRNAs, *Nature* 432 (2004) 235–240.
- [38] H. Wu, H. Xu, L.J. Miraglia, S.T. Crooke, Human RNase III is a 160-kDa protein involved in preribosomal RNA processing, *J. Biol. Chem.* 275 (2000) 36957–36965.
- [39] D. Weidensdorfer, N. Stohr, A. Baude, M. Lederer, M. Kohn, A. Schierhorn, S. Buchmeier, E. Wahle, S. Huttelmaier, Control of c-myc mRNA stability by IGF2BP1-associated cytoplasmic RNPs, *RNA* 15 (2009) 104–115.
- [40] C. Plasencia, E. Martinez-Balibrea, A. Martinez-Cardus, D.I. Quinn, A. Abad, N. Neamati, Expression analysis of genes involved in oxaliplatin response and development of oxaliplatin-resistant HT29 colon cancer cells, *Int. J. Oncol.* 29 (2006) 225–235.
- [41] S.R. Ellis, J.M. Lipton, Diamond Blackfan anemia: a disorder of red blood cell development, *Curr. Top. Dev. Biol.* 82 (2008) 217–241.
- [42] L. Pajor, J.G. Bauman, Flow cytometric measurement of rRNA levels detected by fluorescent in situ hybridization in differentiating K-562 cells, *Histochemistry* 96 (1991) 73–81.
- [43] A. de Capoa, A. Baldini, P. Marlekaj, R. Gambari, G. Raschella, A. Fantoni, Cytologic evidence for increased rRNA gene activity in hemin-induced K562(S) cells, *Cancer Genet. Cytogenet.* 17 (1985) 113–122.
- [44] J.A. Grasso, N.C. Chromey, C.F. Moxey, Biochemical characterization of RNA and protein synthesis in erythrocyte development, *J. Cell Biol.* 73 (1977) 206–222.
- [45] J. van Riggelen, A. Yetil, D.W. Felsner, MYC as a regulator of ribosome biogenesis and protein synthesis, *Nat. Rev. Cancer* 10 (2010) 301–309.
- [46] T. Kondo, N. Minamino, T. Nagamura-Inoue, M. Matsumoto, T. Taniguchi, N. Tanaka, Identification and characterization of nucleophosmin/B23/numatrin which binds the anti-oncogenic transcription factor IRF-1 and manifests oncogenic activity, *Oncogene* 15 (1997) 1275–1281.
- [47] M. Okuda, H.F. Horn, P. Tarapore, Y. Tokuyama, A.G. Smulian, P.K. Chan, E.S. Knudsen, I.A. Hofmann, J.D. Snyder, K.E. Bove, K. Fukasawa, Nucleophosmin/B23 is a target of CDK2/cyclin E in centrosome duplication, *Cell* 103 (2000) 127–140.

- [48] M. Okuwaki, K. Matsumoto, M. Tsujimoto, K. Nagata, Function of nucleophosmin/B23, a nucleolar acidic protein, as a histone chaperone, *FEBS Lett.* 506 (2001) 272–276.
- [49] Y. Yu, L.B. Maggi Jr., S.N. Brady, A.J. Apicelli, M.S. Dai, H. Lu, J.D. Weber, Nucleophosmin is essential for ribosomal protein L5 nuclear export, *Mol. Cell. Biol.* 26 (2006) 3798–3809.
- [50] J. Zlatanova, P. Caiafa, CTCF and its protein partners: divide and rule? *J. Cell Sci.* 122 (2009) 1275–1284.
- [51] K.S. Rees-Unwin, R. Faragher, R.D. Unwin, J. Adams, P.J. Brown, A.M. Buckle, A. Pettitt, C.V. Hutchinson, S.M. Johnson, K. Pulford, A.H. Banham, A.D. Whetton, G. Lucas, D.Y. Mason, J. Burthem, Ribosome-associated nucleophosmin 1: increased expression and shuttling activity distinguishes prognostic subtypes in chronic lymphocytic leukaemia, *Br. J. Haematol.* 148 (2010) 534–543.
- [52] F. Mongelard, P. Bouvet, Nucleolin: a multiFACeTed protein, *Trends Cell Biol.* 17 (2007) 180–186.
- [53] K. Singh, J. Laughlin, P.A. Kosinski, L.R. Covey, Nucleolin is a second component of the CD154 mRNA stability complex that regulates mRNA turnover in activated T cells, *J. Immunol.* 173 (2004) 976–985.